Important note: The present paper work was sent to a scientific journal on 18 October 2021 (it is currently under review).

Topological Design of Tensegrity Structures

Manuel Alejandro Fernández-Ruiz[1,*], Enrique Hernández-Montes[2], Luisa María Gil-Martín[2]

[1]Department of Industrial and Civil Engineering, University of Cádiz (UCA). Campus Bahía de Algeciras, Avda. Ramón Puyol, s/n. 11201 Algeciras (Cádiz), Spain.

[2]Department of Structural Mechanics, University of Granada (UGR). Campus Universitario de Fuentenueva s/n. 18072 Granada, Spain.

[*]manuelalejandro.fernandez@uca.es

ABSTRACT

Tensegrity structures have developed greatly in recent years due to their unique mechanical and mathematical properties. In this work, the topology of the Octahedron family is presented. New tensegrity structures that belong to this family are defined based on their topology. As an example, the eleven-time-expanded octahedron is shown, a super-stable tensegrity formed by 12288 nodes, 6144 struts, and 24576 cables (the largest super-stable tensegrity reported in the literature in terms of number of nodes, cables, and struts so far). The values of the force:length ratios which satisfy the super-stability conditions have also been determined based on the topology of the Octahedron family. Consequently, the computational cost of the process of determining a suitable prestress state and its corresponding equilibrium shape (a process called form-finding) is

significantly reduced. The members of the Octahedron family could have promising engineering and bioengineering applications.

Introduction

Tensegrity structures are spatial structures composed of pre-stressed pin-jointed compression and tension members (struts and cables, respectively) that are self-equilibrated. This type of structure has developed greatly in the last few decades due to their lightweight, ingenious forms, and their controllability and deployability. As a result, tensegrity structures are present in a wide range of scientific fields, such as civil engineering[1,2], robotics[3,4], aerospace,[5–7] and biology[8,9].

The process used to find a self-equilibrated configuration (called a form-finding process) has a key role in the design of tensegrity structures. Tibert and Pellegrino[10] carried out a review of form-finding methods for tensegrity structures. The Force Density Method[11,12] (FDM) and the dynamic relaxation method[13] are the basis of most of these methods. Form-finding methods can be classified into numerical and analytical types. In the literature, there are several pieces of work about numerical form-finding methods[14–17]. On the other hand, only a few analytical form-finding methods can be found[18–20].

The FDM is based on the concept of force:length ratio or force density q[11,12], which is defined as the ratio between the axial force and the length of each member of the tensegrity ($q > 0$ for cables and $q < 0$ for struts). The authors proposed in a previous work an analytical form-finding method of tensegrity structures based on FDM[18,21]. This method consists of finding a set of force:length ratios in a symbolic analysis that achieves an equilibrium shape of the tensegrity structures.

Stability is another key aspect in the design of tensegrity structures. Super-stability is a stability criterion for tensegrity structures with by which the tensegrity is always stable regardless of the level of self-stress and material properties considered[22,23].

The connectivity between the nodes of a tensegrity structure is an input of the form-finding problem. Tensegrity structures can be constructed by using purely geometric intuition based on geometric bodies[20,24,25] or by using topology[21]. A tensegrity family is a group of tensegrity structures that share a common connectivity pattern[21,26,27]. The Octahedron family (presented in Fernández-Ruiz et al.[21]) is composed of the octahedron, the expanded octahedron, and the double-expanded octahedron (see Figure 1). This family has the following properties[21]:

1. The members of the family are composed of rhombic cells.
2. Each member has twice the number of rhombic cells (and consequently, twice the number of nodes, cables and struts) of the previous member of the family.
3. All the inferior members of the family are folded forms in the superior member.
4. Rhombic cells are arranged in three groups.

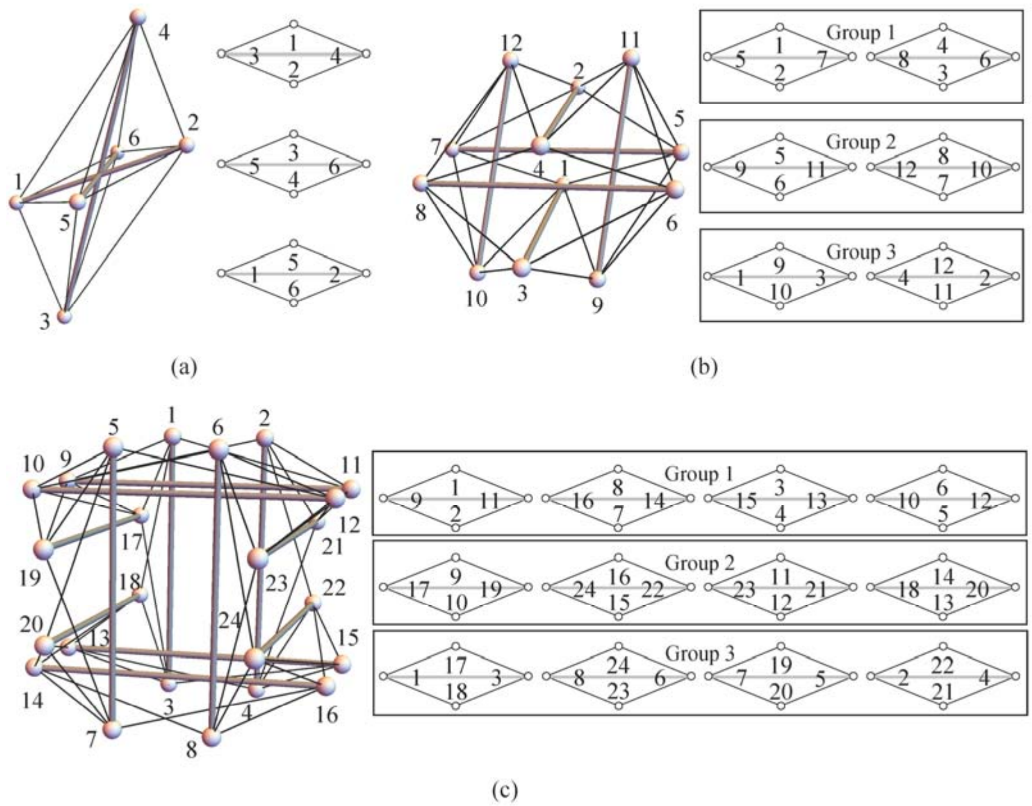

Figure 1. Octahedron (a), expanded octahedron (b) and double-expanded octahedron (c) and their corresponding rhombic cells. Thick gray and thin black lines correspond to struts and cables, respectively

Folded forms are tensegrity structures where some nodes in the equilibrium shape share the same position in the space[18]. On the other hand, full forms are tensegrity structures where all the nodes have different positions in the equilibrium configuration[18].

In the tensegrities of the Octahedron family shown in Figure 1, only two values of force:length ratio are considered: q_c for cables and q_b for bars/struts. The octahedron is the first and simplest member of the Octahedron family (see Figure 1.a). It is composed of 3 rhombic cells, 6 nodes, 3 struts, and 12 cables. The solution given by using the form-finding method[18,21] that leads to a super-stable equilibrium configuration is $q_b = -2q_c$. The second member of the Octahedron family is the expanded octahedron (see Figure 1.b). It is composed of 6 rhombic cells, 12 nodes, 6 struts, and 24 cables. The solutions to the form-finding problem are $q_b = -2q_c$ and $q_b = -3/2q_c$. The solution corresponding to q_b = -

$3/2q_c$ is the super-stable full form of the expanded octahedron (see Figure 1.b). On the other hand, and according to the third property of the Octahedron family, the solution $q_b = -2q_c$ corresponds to the folded form of the expanded octahedron (which is the octahedron whose members are all duplicated). Finally, the third member of the Octahedron family is the double-expanded octahedron (see Figure 1.c). It is composed of 12 rhombic cells, 24 nodes, 12 struts, and 48 cables. In this case, the solutions to the form-finding problem are $q_b = -2q_c$, $q_b = -3/2q_c$ and $q_b = -4/3q_c$. The solution $q_b = -4/3q_c$ corresponds to the super-stable full form of the double-expanded octahedron (see Figure 1.c) and the solutions $q_b = -3/2q_c$ and $q_b = -2q_c$ correspond to the folded forms of the double-expanded octahedron (the expanded octahedron whose members are all duplicated and the octahedron whose members are all quadruplicated, respectively). These results indicate that, at the end of the folding process of an upper member of the Octahedron family, all the struts (and consequently, all the rhombic cells) will overlap each other in the three struts of the first member (the octahedron). For this reason, the cells of all the members of the family always form three groups, which duplicate the number of cells in each expansion. For example: the expanded octahedron has two rhombic cells per group, the double-expanded octahedron has four rhombic cells per group (see Figure 1), and so on.

The basic rhombic cell in the Octahedron family is formed by four nodes connected through four cables and one strut (see Figure 2). The top and bottom nodes are called principal nodes and, as can be seen in Figure 2, they are not connected by the strut. The two nodes connected by the strut are called secondary nodes. The numbering of the rhombic cells corresponding to the three first members of the Octahedron family (the ones known so far) have been obtained by following the connectivity pattern presented in Fernández-Ruiz et al.[21]. It is interesting to notice that the numbering of the nodes in a tensegrity is free, but the connectivity between them has to be kept unchanged.

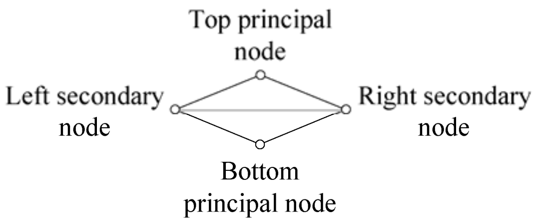

Figure 2. Elementary rhombic cell

The connectivity pattern presented in Fernández-Ruiz et al.[21] can only be applied for the definition of the three first members of the family shown in Figure 1. In this work, the topology of the Octahedron family is completely defined, obtaining all its members without any exceptions. As the first three members of the family are already known, the folding process from a higher member of the family to the previous one is studied. By doing so, the topology of the Octahedron family emerges clearly.

Results

Topology of the Octahedron family

The folding processes from the expanded octahedron to the octahedron and from the double-expanded octahedron to the expanded octahedron are analyzed in detail in order to define the topology of the Octahedron family.

Figure 3.a shows the equilibrium configuration of the expanded octahedron depicted in Figure 1.b with q_b = -2q_c. It is an octahedron whose nodes, struts, and cables are all duplicated. This is because the octahedron is a folded form of the expanded octahedron (or, from another perspective, the expanded octahedron is the expansion of the octahedron). For this reason, there are pairs of nodes that have the same position in the space (see the numbering of nodes in Figure 3.a). It can be seen that struts 5 – 7 and 8 –

6 overlap because nodes 5 – 8 and 7 – 6 have the same coordinates in the space, respectively. Consequently, the struts 5 – 7 and 8 – 6 of Figure 1.b (that are both in group 1) come from the expansion of the strut 3 – 4 of Figure 1.a. Figure 3.b shows the overlapped rhombic cells of the expanded octahedron. Each pair of nodes is composed of two nodes that belong to different rhombic cells (italic and bold numbers, respectively). This distinction has been made based on the rhombic cells shown in Figure 1.b. In Figure 3.c the overlapped rhombic cells are shown separately. Obviously, the rhombic cells shown in Figure 3.c coincide with the ones shown in Figure 1.b.

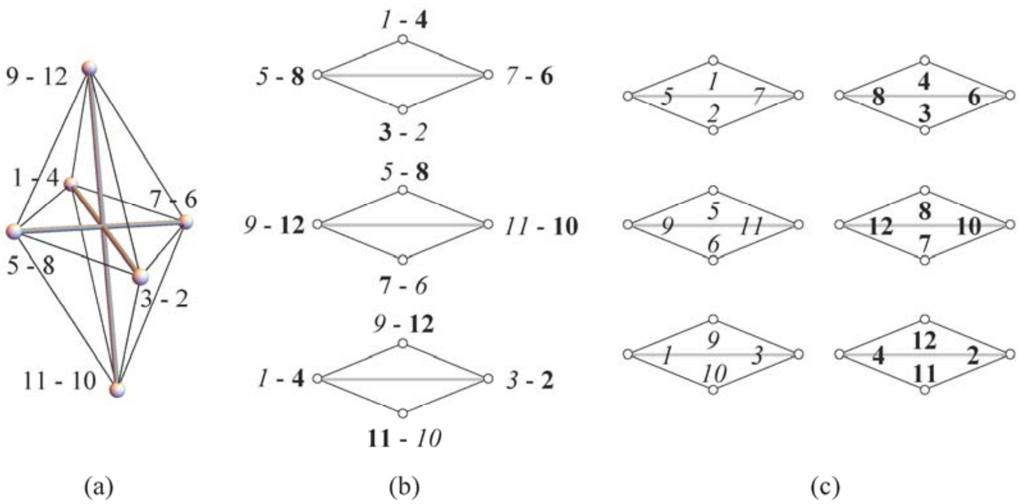

Figure 3. Expanded octahedron with $q_b = -2q_c$ (a), overlapped rhombic cells (b) and rhombic cells (c). Thick gray and thin black lines correspond to struts and cables, respectively.

Figure 4.a shows the equilibrium configuration of the double-expanded octahedron depicted in Figure 1.c with $q_b = -3/2q_c$. It corresponds to an expanded octahedron whose nodes, struts, and cables are all duplicated (see the numbering of nodes of Figure 4.a). In this case, 6 overlapped rhombic cells are shown in Figure 4.b, resulting in 12 rhombic cells (see Figure 4.c). As expected, the rhombic cells in Figure 4.c coincide with the ones in Figure 1.c.

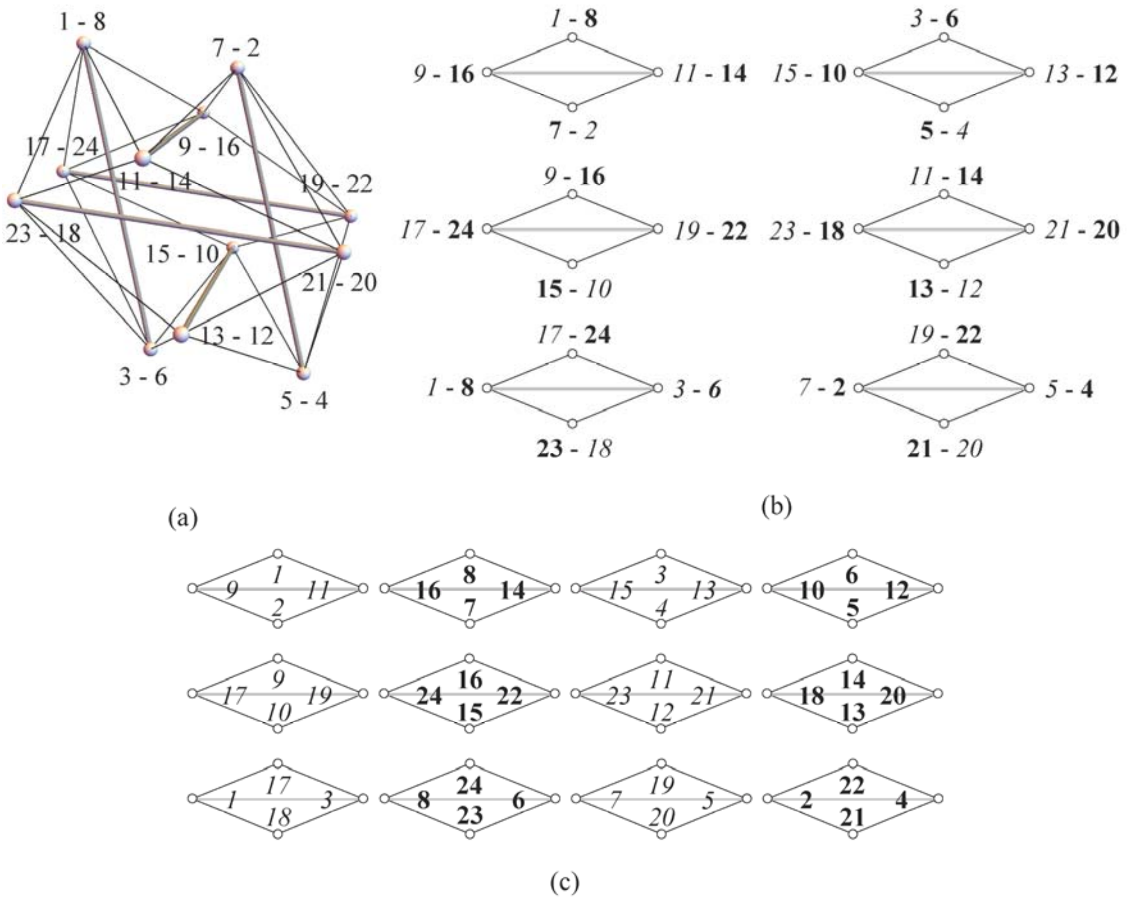

Figure 4. Double-expanded octahedron with $q_b = -3/2q_c$ (a), overlapped rhombic cells (b) and rhombic cells (c). Thick gray and thin black lines correspond to struts and cables, respectively.

Let us consider Figure 3 and 4 from another point of view. Instead of studying the folding of a higher member to a lower one, at this point, the expansion of a lower member to a higher one is considered. Let p be the position of the tensegrity in the Octahedron family (p = 1 for the octahedron, p = 2 for the expanded octahedron, p = 3 for the double-expanded octahedron and so on). Based on Figure 3 and 4, the rhombic cells of ALL the members of the Octahedron family can be obtained by following these steps (with the exception of the octahedron, because it is not the expansion of a previous member of the family):

1. Draw a $3 \times 2^{(p-2)}$ matrix of overlapped rhombic cells.

2. Number consecutively all the pairs of principal nodes of each rhombic cell (see Figure 5.a).
3. From left to right number the secondary nodes as the principal nodes of the following group of rhombic cells in consecutive order from left to right and from top to bottom (see Figure 5.b). Note that the groups of rhombic cells form a closed loop, so group 1 comes after group 3 (see the detail in Figure 5.b).
4. Separate the overlapped rhombic cells so that one rhombic cell is defined by the top-left principal node, by both left secondary nodes and by the bottom-right principal node (see the squared numbers in Figure 5.b). The other rhombic cell is defined by the rest of nodes.

The example shown in Figure 5 corresponds to the expansion of the expanded octahedron to the double-expanded octahedron. The way in which this has been determined is novel: from the expansion of the lower member of the family (expanded octahedron in this case) by following the topology of the Octahedron family.

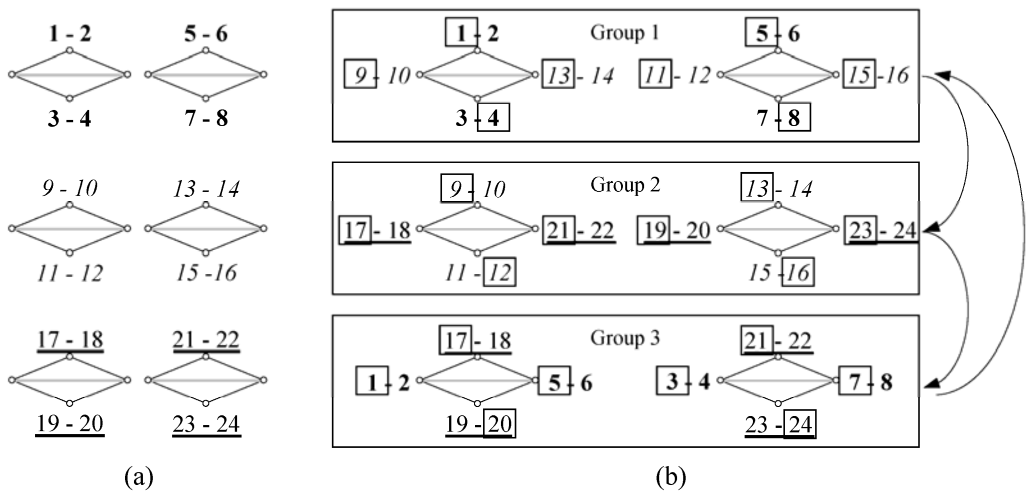

Figure 5. Expansion from the expanded octahedron to the double-expanded octahedron

Superior members of the Octahedron family

Let us apply the topology of the Octahedron family to determine the fourth member: the triple-expanded octahedron (p = 4). The 24 rhombic cells of the triple-expanded octahedron have been defined following the steps described above. The solutions of the form-finding problem are $q_b = -2q_c$, $q_b = -3/2q_c$, $q_b = -4/3q_c$ and $q_b = -5/4q_c$. The solution $q_b = -5/4q_c$ corresponds to the full form of the triple-expanded octahedron (see Figure 6). This is a new super-stable tensegrity composed of 24 rhombic cells, 48 nodes, 24 struts and 96 cables. On the other hand, the solutions $q_b = -4/3q_c$, $q_b = -3/2q_c$ and $q_b = -2q_c$ correspond to the folded forms of the triple-expanded octahedron: the double-expanded octahedron, the expanded octahedron, and the octahedron, respectively. This confirms that this tensegrity belongs to the Octahedron family.

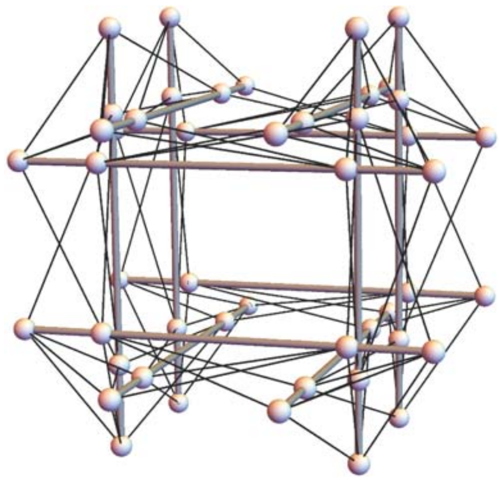

Figure 6. Triple-expanded octahedron

It can be concluded that this newly presented topology represents a general pattern that extends the connectivity pattern previously defined in Fernández-Ruiz et al.[21]. Moreover, the topology of the Octahedron family can be easily programmed in order to define the numbering of the rhombic cells of superior members.

Sequence of solutions

For the sake of clarity and without loss of generality, in all the tensegrities shown in this work, only two force:length ratios have been considered (q_c for cables and q_b for bars/struts). The analytical form-finding method proposed in[18,21] has been used to compute the force:length ratios that lead to an equilibrium configuration of the tensegrity. The biggest computing cost of the form-finding problem corresponds to the analytical calculation of q_c and q_b.

The solutions to the form-finding problem of the full forms of the members of the Octahedron family are $q_b = -2q_c$ for the octahedron, $q_b = -3/2q_c$ for the expanded octahedron, $q_b = -4/3q_c$ for the double-expanded octahedron and $q_b = -5/4q_c$ for the triple-expanded octahedron (all of which are super-stable tensegrities). It can be seen that the force:length ratios of the tensegrities of the Octahedron family follow the mathematical sequence shown in Eq. (1) and depicted in Figure 7.

$$\frac{q_b}{q_c} = -\frac{p+1}{p} \tag{1}$$

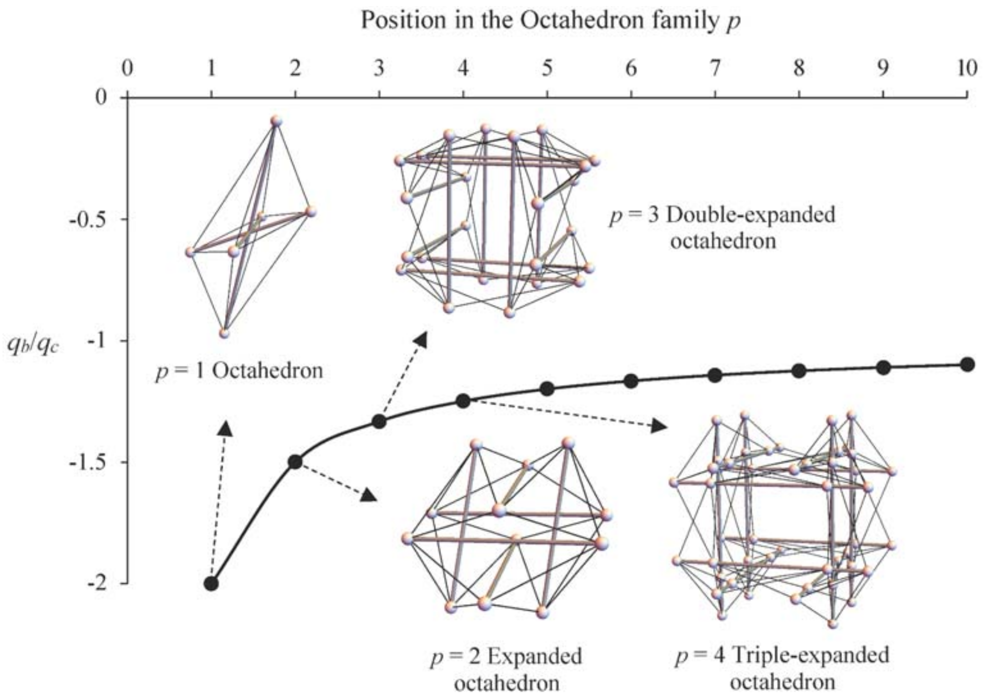

Figure 7. Sequence of solutions of q_b/q_c of the Octahedron family shown in Eq. (1)

It has been proved that the sequence shown in Eq. (1) is valid for all the members of the Octahedron family. Figure 8 shows the equilibrium configurations of the five-time-expanded octahedron, six-time-expanded octahedron, nine-time-expanded octahedron, and eleven-time-expanded octahedron (all of them super-stable). It should be highlighted that the eleven-time-expanded octahedron shown in Figure 8.d is a super-stable tensegrity formed by 12288 nodes, 6144 struts and 24576 cables. As far as the authors know, a super-stable tensegrity with such a high number of nodes, struts, and cables has not been reported in the literature. Moreover, the procedure presented in this paper allows an endless number of new super-stable tensegrities based on the topology of the Octahedron family to be obtained.

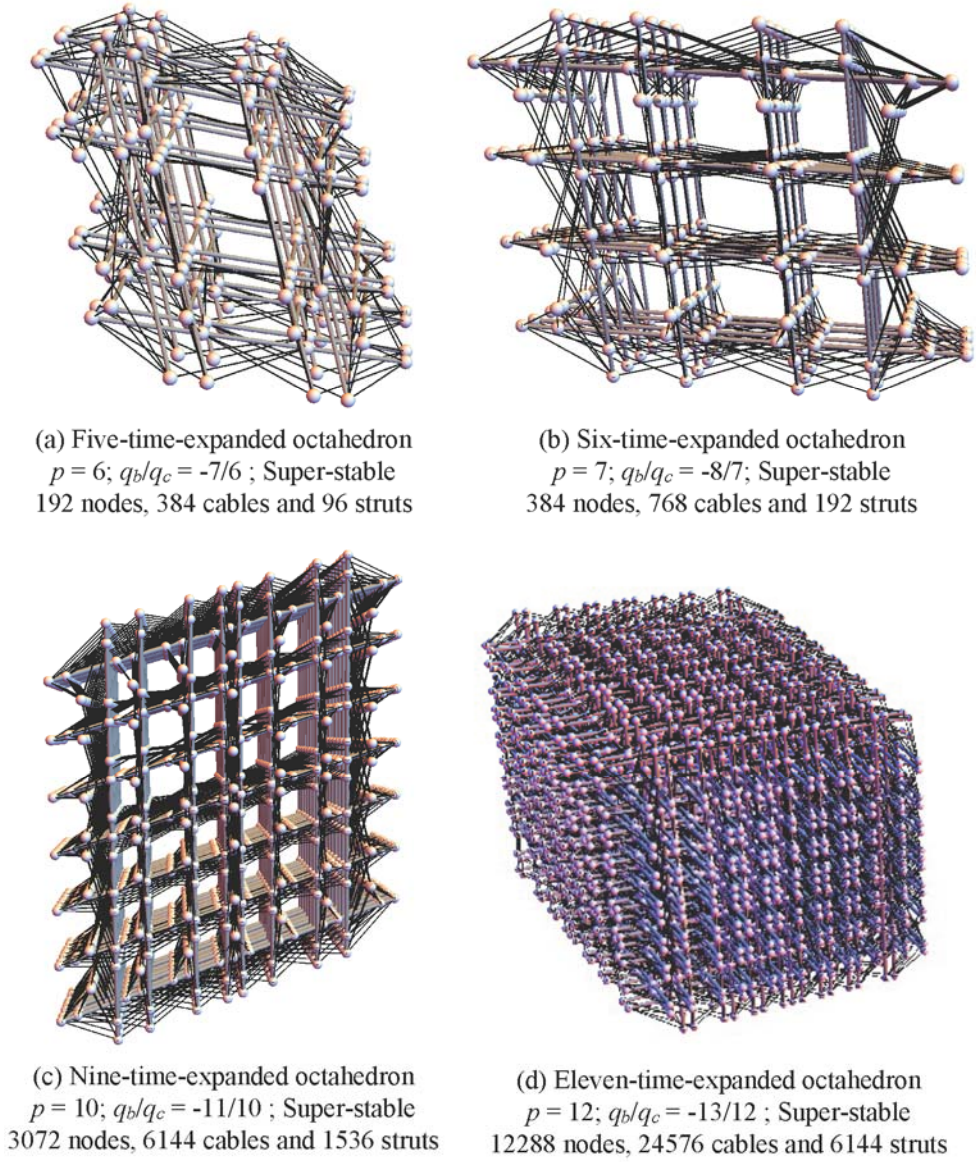

Figure 8. Five-time-expanded octahedron (a), six-time-expanded octahedron (b), nine-time-expanded octahedron (c), and eleven-time-expanded octahedron (d)

It can be seen in Figure 8 that the superior members of the Octahedron family have a quasiregular square honeycomb shape. Honeycomb materials have high strength, specific stiffness, and energy absorption efficiency[28–30] and they are widely observed in natural materials[31]. Due to these characteristics, the members of the Octahedron family such as the eleven-time-expanded octahedron could have promising engineering and bioengineering applications.

Discussion

The topology of the Octahedron family is completely developed. Up to now, only three members of the Octahedron family were known: the octahedron, the expanded octahedron and the double-expanded octahedron. The folding process from a higher member to a lower one has been analyzed in order to define the topology of the family. The topology presented in this work has been adapted to the definition of all the members of the Octahedron family. An analytical form-finding method has been used to compute the equilibrium configuration of the studied tensegrities. It is remarkable that no nodal coordinates or nodal connectivity are required as initial input data, only the position of the tensegrity in the Octahedron family p. The ratio between the force:length ratio of struts and cables (q_b/q_c) that leads to a super-stable equilibrium configuration of the members of the family follows a mathematical sequence that depends on p. Therefore, the computation cost of the analytical form-finding method is significantly diminished (it is reduced to the calculation of the eigenvectors of the force density matrix of the tensegrity). The eleven-time-expanded octahedron is depicted to illustrate the potential of the Octahedron family. This super-stable tensegrity is formed by 12288 nodes, 6144 struts, and 24576 cables, and it is, the largest super-stable tensegrity reported in the literature (in terms of number of nodes, cables, and struts) so far. By applying the procedure presented in this paper, superior members of the Octahedron family can be defined. Finally, due to their quasiregular honeycomb shape, the members of the Octahedron family could have promising engineering and bioengineering applications.

Methods

Analytical form-finding method for tensegrity structures[18,21]

The equilibrium equations of a tensegrity with n nodes and m members can be formulated as[14,32]:

$$\begin{aligned}\mathbf{D}\,\mathbf{x} &= 0\\ \mathbf{D}\,\mathbf{y} &= 0\\ \mathbf{D}\,\mathbf{z} &= 0\end{aligned} \tag{2}$$

where $\mathbf{D} = \mathbf{C}^{\mathrm{T}}\mathbf{Q}\mathbf{C}$ ($\in\Re^{n\times n}$) is the force density matrix and $\mathbf{x}$, $\mathbf{y}$, $\mathbf{z}$ ($\in\Re^{n}$) the nodal coordinate vectors. The symbol $[]^{\mathrm{T}}$ represents the transpose operation of a matrix or vector. The force:length ratio q of each member of the family and the connectivity matrix $\mathbf{C}$ are the inputs of the form-finding method. The connectivity matrix $\mathbf{C}$ ($\in\Re^{m\times n}$) shows the connectivity between the nodes of the tensegrity and it is constructed in the following way: if a general member j connects nodes i and k (with $i < k$), the ith and kth elements of the jth row of $\mathbf{C}$ are set to 1 and -1 respectively. The values of the force:length ratio of each member are collected in the vector $\mathbf{q} = (q_1, q_2, ..., q_m)$ ($\in\Re^{m}$), being $\mathbf{Q}$ the diagonal square matrix of vector $\mathbf{q}$.

A necessary condition for the development of a tensegrity with dimension d is that the rank deficiency of matrix $\mathbf{D}$ is at least $d + 1$ (non-degeneracy condition[15,18]). The non-degeneracy condition is achieved imposing that the characteristic polynomial of $\mathbf{D}$ (see Eq. (3)) has $d + 1$ zero roots. By doing so, coefficients a_3, a_2, a_1 and a_0 of the characteristic polynomial must be zero in order to obtain a three-dimensional (3D) tensegrity. By construction of $\mathbf{D}$, it is always singular and consequently coefficient a_0 is always 0. The system of equations in terms of the force:length ratios of the members of the 3D tensegrity shown in Eq. (4) is analytically solved in order to obtain a rank deficiency of matrix $\mathbf{D}$ of at least $d + 1$.

$$p(\lambda)=\lambda^{n}+a_{n-1}\lambda^{n-1}+\ldots+a_1\lambda+a_0 \tag{3}$$

$$
\begin{aligned}
&a_3(q_1,\ldots,q_{\mathrm{m}}) = 0\\
&a_2(q_1,\ldots,q_{\mathrm{m}}) = 0\\
&a_1(q_1,\ldots,q_{\mathrm{m}}) = 0
\end{aligned}
\tag{4}
$$

A more detailed description of the analytical form-finding procedure used in this work can be seen in[18,21].

The highest computation cost of the form-finding method is the computation of the analytical solution of the system of equations shown in Eq. (4). The sequence of solutions of q_b/q_c followed by the members of the Octahedron family means that this step can be avoided. In addition, matrix **D** can be directly formulated using the values of the force:length ratio of the members as:

$$
\mathbf{D}_{ij} = \begin{cases} \sum_{k\in\Gamma} q_k & \text{for } i = j \\ -q_k & \text{if nodes } i \text{ and } j \text{ are connected by member } k \\ 0 & \text{otherwise} \end{cases}
\tag{5}
$$

With Γ as the set of members connected to the node *i*. Consequently, the form-finding process of the members of the Octahedron family is reduced to a calculation of the eigenvectors of **D** (Eq. (2)).

A super-stable tensegrity is always stable, regardless of material properties and prestress[22,23]. The super-stability conditions of tensegrity structures are as follows[22,23,32]:

1. The rank deficiency of the force density matrix **D** is exactly $d + 1$.
2. The force density matrix **D** is positive semi-definite.
3. The rank of the matrix **G** is $(d^2 + d)/2$.

An in-depth explanation on the geometry matrix **G** can be seen in[32]. The stability of tensegrity structures has been discussed in detail in [21,23,32]. All the full forms of the members of the Octahedron family presented in this work fulfills all the super-stability conditions.

References

1. Rhode-Barbarigos, L., Hadj Ali, N. B., Motro, R. & Smith, I. F. C. Designing tensegrity modules for pedestrian bridges. *Eng. Struct.* **32**, 1158–1167 (2010).
2. Skelton, R. E., Fraternali, F., Carpentieri, G. & Micheletti, A. Minimum mass design of tensegrity bridges with parametric architecture and multiscale complexity. *Mech. Res. Commun.* **58**, 124–132 (2014).
3. Liu, S., Li, Q., Wang, P. & Guo, F. Kinematic and static analysis of a novel tensegrity robot. *Mech. Mach. Theory* **149**, 103788 (2020).
4. Wang, Z., Li, K., He, Q. & Cai, S. A light-powered ultralight tensegrity robot with high deformability and load capacity. *Adv. Mater.* **31**, 1806849 (2019).
5. Chen, M., Goyal, R., Majji, M. & Skelton, R. E. Design and analysis of a growable artificial gravity space habitat. *Aerosp. Sci. Technol.* **106**, 106147 (2020).
6. Liu, K., Wu, J., Paulino, G. H. & Qi, H. J. Programmable Deployment of Tensegrity Structures by Stimulus-Responsive Polymers. *Sci. Rep.* **7**, 1–8 (2017).
7. Wang, Y. T., Liu, X. N., Zhu, R. & Hu, G. K. Wave propagation in tunable lightweight tensegrity metastructure. *Sci. Rep.* **8**, 1–12 (2018).
8. Ingber, D. E. The Architecture of Life. *Sci. Am.* **278**, 48–57 (1998).
9. Scarr, G. *Biotensegrity: The structural basis of life*. (2014).
10. Tibert, A. G. & Pellegrino, S. Review of Form-Finding Methods for Tensegrity Structures. *Int. J. Sp. Struct.* **18**, 209–223 (2003).
11. Linkwitz, K. & Schek, H. J. Einige Bemerkungen zur Berechnung von vorgespannten Seilnetzkonstruktionen. *Ingenieur-Archiv.* **40**, 145–158 (1971).
12. Schek, H. J. The force density method for form-finding and computation of general networks. *Comput. Methods Appl. Mech. Eng.* **3**, 115–134 (1974).

13. Otter, J. R. H. Computations for prestressed concrete reactor pressure vessels using dynamic relaxation. *Nucl. Struct. Eng.* **1**, 61–75 (1965).

14. Tran, H. C. & Lee, J. Advanced form-finding of tensegrity structures. *Comput. Struct.* **88**, 237–246 (2010).

15. Zhang, J. Y. & Ohsaki, M. Adaptive force density method for form-finding problem of tensegrity structures. *Int. J. Solids Struct.* **43**, 5658–5673 (2006).

16. Estrada, G. G., Bungartz, H.-J. & Mohrdieck, C. Numerical form-finding of tensegrity structures. *Int. J. Solids Struct.* **43**, 6855–6868 (2006).

17. Masic, M., Skelton, R. E. & Gill, P. E. Algebraic tensegrity form-finding. *Int. J. Solids Struct.* **42**, 4833–4858 (2005).

18. Hernández-Montes, E., Fernández-Ruiz, M. A., Gil-Martín, L. M., Merino, L. & Jara, P. Full and folded forms: a compact review of the formulation of tensegrity structures. *Math. Mech. Solids* **23**, 944–949 (2018).

19. Vassart, N. & Motro, R. Multiparameted form-finding method: application to tensegrity systems. *Int. J. Sp. Struct.* **14**, 89–104 (1999).

20. Zhang, L. Y., Li, Y., Cao, Y. P. & Feng, X. Q. A unified solution for self-equilibrium and super-stability of rhombic truncated regular polyhedral tensegrities. *Int. J. Solids Struct.* **50**, 234–245 (2013).

21. Fernández-Ruiz, M. A., Hernández-Montes, E., Carbonell-Márquez, J. F. & Gil-Martín, L. M. Octahedron family: The double-expanded octahedron tensegrity. *Int. J. Solids Struct.* **165**, 1–13 (2019).

22. Connelly, R. Tensegrity structures. Why are they stable? in *Rigidity theory and applications* (eds. Thorpe, M. F. & Duxbury, P. M.) 47–54 (Kluwer Academic / Plenum Publishers, 1998).

23. Zhang, J. Y. & Ohsaki, M. Stability conditions for tensegrity structures. *Int. J.

Solids Struct. **44**, 3875–3886 (2007).

24. Li, Y., Feng, X. Q., Cao, Y. P. & Gao, H. Constructing tensegrity structures from one-bar elementary cells. *Proc. R. Soc. A Math. Phys. Eng. Sci.* **466**, 45–61 (2010).
25. Zhang, L. Y., Li, Y., Cao, Y. P., Feng, X. Q. & Gao, H. Self-equilibrium and super-stability of truncated regular polyhedral tensegrity structures: A unified analytical solution. *Proc. R. Soc. A Math. Phys. Eng. Sci.* **468**, 3323–3347 (2012).
26. Fernández-Ruiz, M. A., Hernández-Montes, E. & Gil-Martín, L. M. The Z-octahedron family: A new tensegrity family. *Eng. Struct.* **222**, 111151 (2020).
27. Fernández-Ruiz, M. A., Hernández-Montes, E. & Gil-Martín, L. M. The Octahedron family as a source of tensegrity families: The X-Octahedron family. *Int. J. Solids Struct.* **208**–**209**, 1–12 (2021).
28. Jiang, W. *et al.* Electromagnetic wave absorption and compressive behavior of a three-dimensional metamaterial absorber based on 3D printed honeycomb. *Sci. Rep.* **8**, 1–7 (2018).
29. Tao, Y. *et al.* Mechanical properties and energy absorption of 3D printed square hierarchical honeycombs under in-plane axial compression. *Compos. Part B Eng.* **176**, 107219 (2019).
30. Wang, Z. Recent advances in novel metallic honeycomb structure. *Compos. Part B Eng.* **166**, 731–741 (2019).
31. Zhang, Q. *et al.* Bioinspired engineering of honeycomb structure - Using nature to inspire human innovation. *Prog. Mater. Sci.* **74**, 332–400 (2015).
32. Zhang, J. Y. & Ohsaki, M. *Tensegrity Structures. Form, Stability, and Symmetry*. (Springer, 2015).

Author contributions

M.A.F.R.: Conceptualization, Methodology, Writing - original draft. E.H.M.: Supervision, Investigation. L.M.G.M.: Supervision, Investigation, Writing - review & editing.

Additional information

Competing Interests: The authors declare that they have no competing interests.

Figure legends

Figure 1. Octahedron (a), expanded octahedron (b) and double-expanded octahedron (c) and their corresponding rhombic cells. Thick gray and thin black lines correspond to struts and cables, respectively.

In Figure 1, all the members of the Octahedron family known so far are shown: the octahedron, the expanded octahedron and the double-expanded octahedron. These tensegrities can be constructed by assembling one-bar elementary rhombic cells. The rhombic cells that conform each tensegrity are also presented in the figure, where thick gray and thin black lines correspond to struts and cables, respectively. Rhombic cells are grouped in three main groups because all of them will overlap each other in the three struts of the first member (the octahedron). Finally, numbering of nodes is also shown in order to make clear that the connectivity between the nodes of the tensegrity is completely defined by the rhombic cells.

Figure 2. Elementary rhombic cell

In this figure the nomenclature of the nodes of a rhombic cell is defined: top and bottom principal nodes and left and right secondary nodes.

Figure 3. Expanded octahedron with q_b = -2q_c (a), overlapped rhombic cells (b) and rhombic cells (c). Thick gray and thin black lines correspond to struts and cables, respectively

Figure 3.a shows the equilibrium configuration of the expanded octahedron with $q_b = -2q_c$. This solution leads to a folded form: an octahedron whose nodes, cables and struts are all duplicated. Figure 3.b shows the overlapped rhombic cells of the resultant tensegrity. The pairs of nodes indicated in Figure 3.b correspond to two nodes that share the same position in the space. Italic and bold numbers indicate that their corresponding nodes belong to different rhombic cells. Figure 1.b has been used in order to make this distinction. Finally, Figure 3.c shows the rhombic cells that conform the folded form of the expanded octahedron.

Figure 4. Double-expanded octahedron with q_b = -3/2q_c (a), overlapped rhombic cells (b) and rhombic cells (c). Thick gray and thin black lines correspond to struts and cables, respectively.

Figure 4.a shows the equilibrium configuration of the double-expanded octahedron with $q_b = -3/2q_c$. This solution leads to a folded form: an expanded octahedron whose nodes, cables and struts are all duplicated. On the other hand, Figure 4.b shows the overlapped rhombic cells of the folded form of the double-expanded octahedron. As in Figure 3, the pairs of nodes indicated in Figure 4.b correspond to two nodes that share the same position in the space. Italic and bold numbers indicate that their corresponding nodes belong to different rhombic cells. Figure 1.c has been used in order to make this distinction. Finally, Figure 4.c shows the rhombic cells that conform the folded form of the double-expanded

octahedron.

Figure 5. Expansion from the expanded octahedron to the double-expanded octahedron

The procedure proposed in this work to obtain the rhombic cells of all the members of the Octahedron family is applied in Figure 5 to the double-expanded octahedron (p = 2). In Figure 5.a the principal nodes of the overlapped rhombic cells are numbered. It is interesting to remark that the numbering of these nodes is free. Figure 5.b shows the numbering of the secondary nodes, that is directly influenced by the numbering of the principal nodes, following the topology of the Octahedron family. Finally, the overlapped rhombic cells are separated (squared numbers in Figure 5.b).

Figure 6. Triple-expanded octahedron

Figure 6 shows the equilibrium configuration of the triple-expanded octahedron. The rhombic cells that conform this tensegrity have been obtained according to the topology of the Octahedron family.

Figure 7. Sequence of solutions of q_b/q_c of the Octahedron family shown in Eq. (1)

Figure 7 shows the graphical representation of the sequence of solutions of q_b/q_c of the Octahedron family (see Eq. (1)). This sequence of solutions is a very important contribution of the work because it significantly reduces the computation cost of the form-finding process.

Figure 8. Five-time-expanded octahedron (a), six-time-expanded octahedron (b), nine-time-expanded octahedron (c), and eleven-time-expanded octahedron (d)

Figure 8 shows the equilibrium shapes of the five-time-expanded octahedron, six-time-expanded octahedron, nine-time-expanded octahedron, and eleven-time-expanded octahedron. These members of the Octahedron family have been obtained following the procedure proposed in this work. It should be noted that, as far as the authors know, the eleven-time-expanded octahedron is the largest super-stable tensegrity structure reported in literature.